Available online at www.sciencedirect.com
SCIENCE DIRECT®
Chemical Physics Letters 423 (2006) 366–370
CHEMICAL PHYSICS LETTERS
www.elsevier.com/locate/cplett

Planar doping of crystalline fullerene with cobalt

Vasily Lavrentiev [a,b,*], Hiroshi Naramoto [a], Kazumasa Narumi [a], Seiji Sakai [a], Pavel Avramov [a]

[a] Advanced Science Research Center, Japan Atomic Energy Agency, Takasaki-branch, 1233 Watanuki, Takasaki, Gunma 370-1292, Japan
[b] INTERCI, Independent Scientific Center, Kirova Str. 36-11, Sumy 40030, Ukraine

Received 30 December 2005; in final form 11 March 2006
Available online 6 April 2006

Abstract

A study of 100 keV Co^+-implanted C_{60} films with Rutherford Backscattering and Raman spectroscopy has revealed the pronounced cobalt translation from the surface layer of amorphous carbon into the deeper crystalline fullerene due to post-implantation annealing at 300 °C. Carbon density gradient along the film depth is discussed as a driving force of this effect. Cobalt deficit in the doped fullerene layer, detected by means of ion beam analysis, suggests ionization of the C_{60} molecules under the collisions with 2 MeV He^+ ions.

1. Introduction

Evaluation of the C_{60} electronic properties, reported in recent past [1], reveals doping of this material with metals as attractive channel of modern material science. The importance of this procedure has been recognized after the successful studies of the alkali metal (A)-fullerene compounds. The experiments have revealed electrical conductivity of the compounds related with filling unoccupied t_{1u}-derived states [2–4]. Following discovery of A_xC_{60} superconductivity with relatively high critical temperature (up to 33 K) has improved an importance of the problem, suspecting many promising metal–C_{60} combinations [5–8]. However, the conventional doping procedure, exploited during AC_{60} creation [4–7], becomes useless for many other metals due to high sublimation heat of those, requiring extreme thermal conditions. From this viewpoint, ion implantation as possible doping method has the evident advantages, such as: temperature independence and controllability of the process, creation of shallow doped layer that are important points during device manufacturing [9]. Concerning to the fullerene doping, moreover, ion implantation is implied to be especially attractive due to insensitivity of the resulting structure to oxygen [10]. On the other hand, testing ion implantation to fullerene has revealed destroying C_{60} molecules [10–15] that sufficiently restricts the interest to this technique. In spite of this problem, we have applied ion implantation for doping of crystalline fullerene with cobalt. Analysis of the previous results shows the enhanced penetration of potassium during K^+ implantation into C_{60} at elevated temperatures [10]. Suspecting the way for C_{60} doping, we have tried to check this phenomenon using post-implantation annealing of cobalt-implanted fullerene.

2. Experiment

High-pure C_{60} has been deposited on clean sapphire substrate at 450 °C Knudsen cell temperature in ultra-high vacuum. Final thickness of the deposited C_{60} films was about 1000 nm. According to our experience, the applied conditions lead to formation of the nano-crystalline C_{60} films with fcc crystal lattice. The fullerene films have been implanted with 100 keV Co^+ ions at room temperature (RT) in ultra-high vacuum. The conventional ion implantation provided uniform distribution of the dopant along the 5×5 mm^2 sample surface owing to the beam scanning. The ion beam current was equal to 1 μA at the beam spot of about 1 mm. The implantation dose was varied in the inter-

* Corresponding author.
E-mail address: vlavren@mail.ru (V. Lavrentiev).

0009-2614/$ - see front matter © 2006 Elsevier B.V. All rights reserved.
doi:10.1016/j.cplett.2006.03.087

val of 1×10^{12} –5×10^{16} Co/cm^2. We applied Rutherford backscattering spectroscopy (RBS) with 2 MeV He^+ beam to analyze the chemical composition of the implanted films. During the RBS analysis ion beam current was kept at 10 nA. To convert the RBS spectra into cobalt depth profiles we have used RUMP code (RBS Universal Master Package, RUMP) [16,17]. Several etalon-samples have been used (C, Al, Si, Cu and Au) for accurate energy scale calibration of the RBS spectra that was important point in correct determination of the dopant depth position. As general, the RUMP simulation method has included the search of much suitable composition in set of the layers, modeling the doped sample, to fit precisely the experimental RBS spectrum by theoretical one. Correlation between ion doses, taken from the experimental setup and from the simulation of as-implanted sample RBS spectrum, was a criterion of the correct RUMP application. Additionally, we have modeled the dopant depth profile in the as-implanted samples with a TRIM code. As known, TRIM (Transport of ions in matter) [16,18] is a power tool for determination of the ion range distribution for given ion-target combination. A correspondence of the models and the experimental profiles, taken for the as-implanted samples, was another criterion during RUMP exploitation. To elucidate the temperature effect on dopant distribution we applied annealing of the implanted samples at 300 °C in vacuum. Potassium ion implantation into fullerene at this temperature provided deepest penetration of the dopant [10]. Before the experiments (ion implantation, post-implantation annealing and ion-beam analysis) the samples have been kept in the dry atmosphere under normal conditions. Chemical state of carbon before and after ion implantation was controlled by Raman spectrometry, using nanobeam of argon laser with 488 nm wavelength and 0.5 mW beam power. To avoid the structure deviation under the laser beam exposition we used scanning mode during the Raman measurements, decreasing a probe time at one point up to 25 ms.

3. Results and discussion

It was reported that ion implantation of potassium into C_{60} film with ion energy of several tens keV transforms the surface layer of fullerene into amorphous carbon [10–12]. Apparently, the dopant was situated mainly within amorphous carbon. However, the unusual depth profile of potassium, implanted in fullerene film under the elevated temperatures [10], suggests penetration of potassium into undestroyed C_{60} layer. We aimed to check the temperature effect, providing cobalt ion implantation into fullerene. In order to elucidate an importance of temperature in the unusual dopant distribution, we have separated the implantation and thermal effects in time, preparing cobalt ion implantation and post-implantation annealing of the samples, consequently.

First of all, we have tried to confirm the destruction of C_{60} molecules due to 100 keV Co^+ implantation. Fig. 1 shows the Raman spectra of the fullerene films implanted with various doses. It is seen that Raman spectra of the implanted samples include a broad peak between 900 and 1800 cm^{-1}, indicating formation of amorphous carbon (a-C). It was found that a-C peak rises after implantation with ion dose higher then 10^{13} Co/cm^2. Gradual reduction of the main C_{60} peak at 1468 cm^{-1} with ion dose is referred to the contribution from the deeper layer of undestroyed fullerene [10].

In order to confirm the dopant location in as-implanted fullerene we have prepared the RBS spectra of the samples. The spectrum of the fullerene film implanted with ion dose of 3×10^{16} cm^{-2} is shown in Fig. 2a. The spectrum reveals carbon edge at lower channels and evident peak at about 415 channel related with implanted cobalt. Small feature nearby the carbon edge reflects some contamination of the sample surface with oxygen generally detected in the implanted fullerene films [10,12]. Fig. 2b depicts the respective cobalt depth profile simulated with RUMP. The simulation yields a projected range (R_p) of about 64 nm. Adjusting the cobalt depth profile with that, simulated by TRIM, gives us the carbon density in the surface layer along ion range close to 2.45 g/cm^3. This value is much higher than average density of the crystalline fullerene and little above than that for graphite (1.7 and 2.23 g/cm^3, respectively [1]). Apparently, the evaluated density should be referred to a-C, creating in the surface layer during ion implantation.

The surface layer density has been also estimated from analysis of Raman data. Fig. 3 shows the Raman spectrum of the implanted fullerene film, including analysis of a-C peak as superposition of two Lorentzians (so-called D and G peaks [19]). Using the semiempirical model of amorphization trajectory [19] and ratio of the D and G peak intensities ($I_D/I_G = 0.7$), the implanted layer was defined as highly disordered carbon, containing about 14% of sp^3 phase. Such carbon composition has the average density

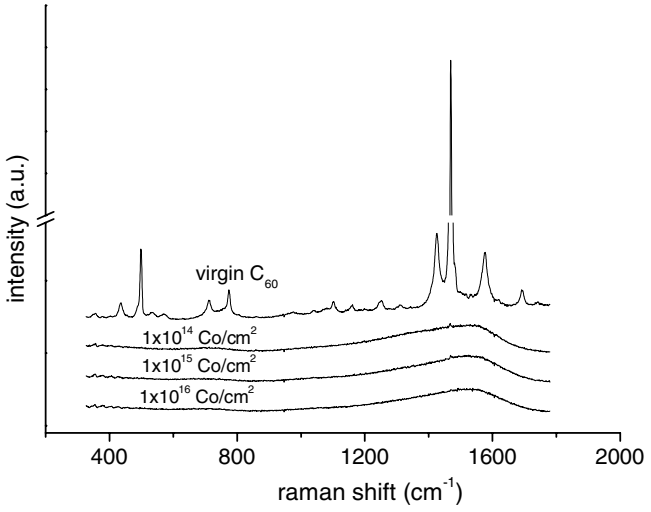

Fig. 1. Raman spectra of C_{60} films virgin and implanted by 100 keV Co^+ ions with various ion doses.

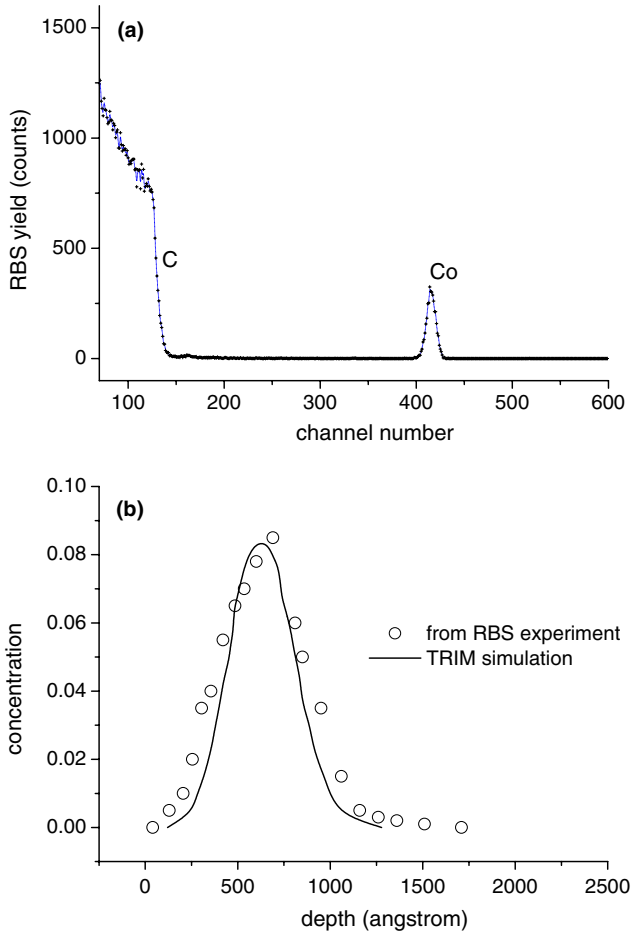

Fig. 2. (a) RBS spectrum of C_{60} film implanted by 100 keV Co^+ ions with ion dose of 3×10^{16} cm^{-2}. (b) The respective depth profile of cobalt in the implanted sample simulated by RUMP code and TRIM simulated depth profile of cobalt after 100 keV Co^+ implantation into amorphous carbon with density of 2.45 g/cm^3.

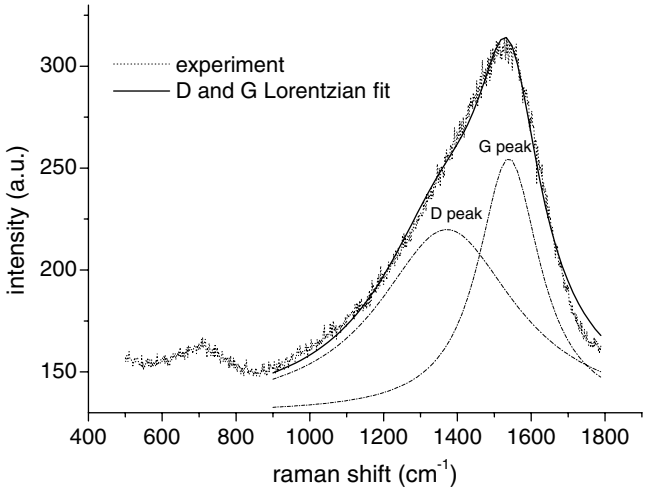

Fig. 3. Separation of the amorphous carbon peak by D and G Lorentz peaks in Raman spectrum of C_{60} film implanted by 100 keV Co^+ with ion dose of 3×10^{16} cm^{-2}.

of 2.4 g/cm^3. It could be seen good correlation of the carbon densities taken with the RBS and Raman spectra that confirms the situation of cobalt in the a-C surface layer.

Therefore, ion implantation of cobalt into fullerene film results in formation of two carbon layers with different densities, i.e. the a-C surface layer, containing implanted cobalt atoms, and deeper layer of virgin C_{60} crystals. This difference happened due to the destruction of C_{60} molecules during ion implantation and following shrinkage of the surface layer. Under such conditions any guest atoms, located in the shrinking layer, should be influenced by driving force related with the carbon density gradient. It means that implanted atoms have to move in direction of the gradient, i.e. from more dense amorphous carbon to more specious fullerene lattice. As a consequence, we found a long tail in the depth distribution of cobalt even in as-implanted sample (see Fig. 2b). This conclusion also elucidates elongation of the dopant depth profiles observed after K^+ implantation into fullerene at elevated temperatures [10]. To check this idea we have studied the cobalt depth distributions after annealing of the implanted C_{60} films.

Fig. 4a displays the RBS spectra of the C_{60} film just after 100 keV Co^+implantation and after following annealing at 300 °C for 2 h. It is seen that after annealing cobalt peak has been shifted to the lower channels, suggesting in-depth cobalt translation during the thermal treatment. Stable position of the C edge after annealing emphasizes the origin of the Co peak shift. Surprising decrease of the peak height after annealing should be interpreted as cobalt losing during the treatment. This phenomenon was also found during the analysis of potassium ion implantation at the elevated temperatures [10], however any explanation has not been done.

Fig. 4b shows the Co depth profiles in the film just after implantation and after subsequent annealing prepared by RUMP simulation of the respective RBS spectra. It is clear that cobalt after annealing is situated in the deeper layer of virgin C_{60} crystals. Evidently, similar doping procedure could be executed for any other metals chemically inactive to carbon.

Features of the in-depth cobalt translation could be understood from the quantitative analysis of the process. Indeed, one-directional motion of the guest atoms in fullerene, occurring at temperature T under the effect of driving force F, can be described by Einstein equation [20]

$$v = \frac{D}{kT}F \tag{1}$$

where v is a velocity of the guest atoms; D is a diffusion coefficient; k is Boltzmann's constant.

It is convenient to imagine another way for the sample treatment to characterize driving force of the cobalt translation. The film modification should be similar, if the surface C_{60} film layer, somehow doped by cobalt along the R_p layer, suddenly to subject to the high in-plane compression up to the molecular crushing. Evidently, the Co atoms, dissolved initially in the surface C_{60} layer, should be squeezing out from the dense layer of disordered carbon into the deeper specious C_{60} layer. The main features of the film, modified in such a way, are the carbon density

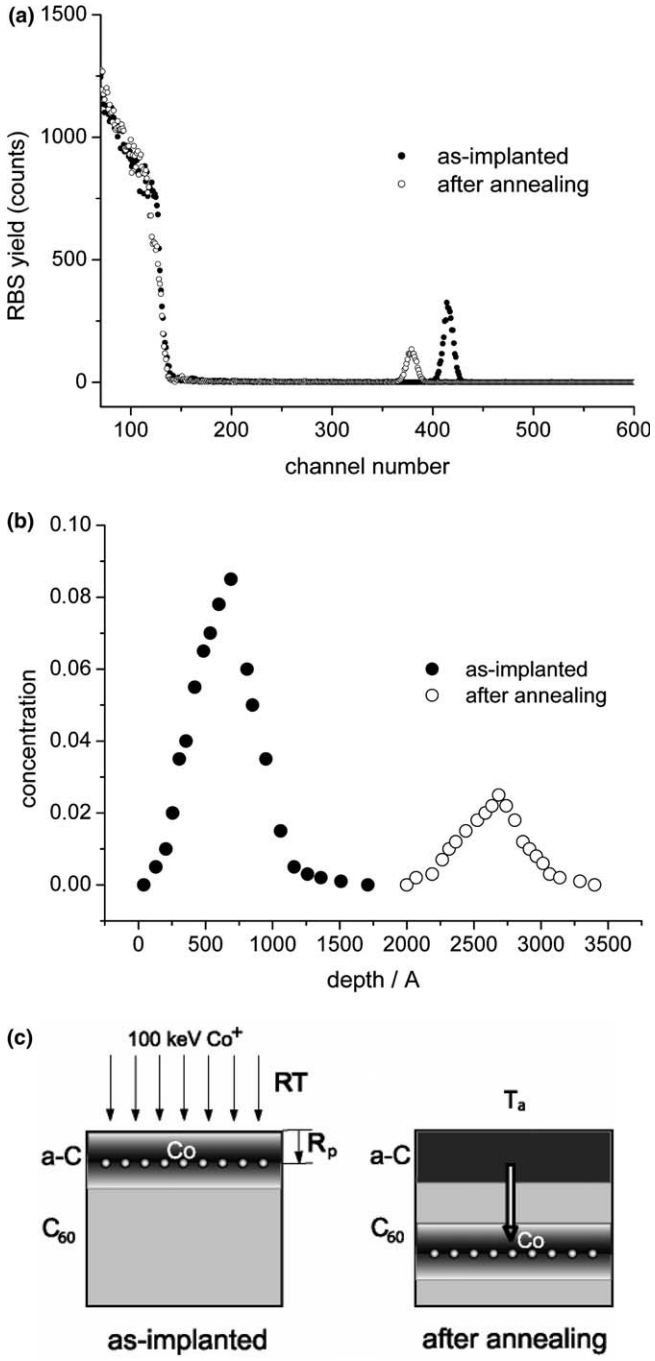

Fig. 4. (a) RBS spectra of C_{60} film after 100 keV Co^+ ion implantation with ion dose of 3×10^{16} cm^{-2} and after post-implantation annealing at 300 °C for 2 h. (b) The respective depth profiles of cobalt in the analyzed sample. (c) The schemes of the cobalt-implanted fullerene sample just after implantation at RT (left) and after following annealing at T_a temperature (right).

gradient, directed into the film depth, and strained state, decreasing gradually the lattice space during out-depth approaching to the surface layer. These features activate the in-depth Co motion.

The force, acting on each guest atom in the strained layer, can be expressed through free energy decrease along the in-depth atomic jump, i.e.

$$F=\frac{\sigma\Omega}{d} \tag{2}$$

where σ is a dilatation stress, arising due to the shrinkage of the surface carbon layer; Ω is the change of unit volume around the jump; d is a jump distance. According to the Hook's law $\sigma = E\varepsilon$, and strain ε can be estimated roughly as $\varepsilon \approx \Delta\rho/\rho_0$, where $\Delta\rho = \rho_a - \rho_0$, ρ_a and ρ_0 are the densities of a-C and solid C_{60}, respectively; E is the fullerene elastic modulus. Taking into account these equations, the velocity of the cobalt in-depth translation v could be defined as

$$v=\frac{D}{kT}\frac{\Delta\rho}{\rho_0}\frac{E\Omega}{d}, \tag{3}$$

that permits us to estimate the diffusion coefficient D of cobalt in crystalline fullerene. From the experiment $v=2.8\times10^{-9}$ cm/s, $T=573$ K, $\Delta\rho=0.75$ g/cm^3, and assuming that $E=18\times10^{10}$ dyn/cm^2 [21], $d\approx3\times10^{-8}$ cm, and $\Omega\approx5\times10^{-23}$ cm^3, we have $D\approx2\times10^{-18}$ cm^2/s. This estimation elucidates a dominant role of the driving force in the cobalt in-depth translation. Minority of the thermal diffusion in this phenomenon prevents broadening of the dopant profile during annealing (see Fig. 4b). Indeed, broadening of the dopant distribution due to the thermal diffusion can be estimated as $\sqrt{Dt}$, where t is the annealing time, that leads to the negligible value of about 1 nm.

The detected effect of the dopant loss after annealing should receive some discussion. It is seen that RBS analysis of the fullerene films just after RT ion implantation reveals adequate content of the dopant. However, if the analysis was executed for the thermally treated samples the experiments show the dopant deficit. Same tendency has been observed after secondary ion mass spectroscopy (SIMS) profiling of the 30 keV K^+-implanted C_{60} films [10]. As reported, SIMS analysis of the film after ion implantation at 300 °C has revealed evident in-depth translation of potassium with 20% of the dopant loss. In the present study RBS analysis of the 100 keV Co^+-implanted C_{60} film after annealing at 300 °C has detected sufficient in-depth translation of the dopant and more then 60% of the cobalt loss (see Fig. 4b). It should be noted that the dopant losing occurs, if the implanted atoms are situated in the deeper C_{60} layer. Since SIMS and RBS are the ion beam techniques, it is reasonable to suspect the ion beam effect in the dopant loss. As known, the collisions of high-energy (several hundreds keV) hydrogen or helium ions with C_{60} molecules result in pronounced ionization of the carbon cages [22,23]. The collisions at higher energy will increase the probability of the electronic excitations [15]. Hence, during 2 MeV He^+ beam analysis of the implanted and annealed sample the C_{60} molecules in a volume of the deeper layer, shaded by ion beam spot, will be ionizing under the collisions with the swift helium ions. The C_{60} ionization should be sensitive for cobalt atoms, situated within fullerene lattice, if those are positively charged. Coulomb interaction with positive C_{60} ions of fullerene lattice will push

cobalt ions out of the analyzing volume. This conclusion leads to the idea that cobalt, located within C_{60} crystals after post-implantation annealing, is also in the ionized state. The Co ionization could be promoted by Co–C_{60} bonding feature, requiring electron transfer from Co atom toward C_{60} molecule [24,25]. If the molecules in Co–C_{60} compound lose binding electrons during the collisions with fast helium ions, the Co–C_{60} bonds can be easily broken due to the Coulomb repulsion. The released Co ions will be removed easily through the specious channels of the ionized C_{60} lattice to the neighboring region, containing only virgin C_{60} molecules. As a result, the detected quantity of the dopant is occurred much lower than expected one. Under the done explanation the dopant loss effect claims that after post-implantation annealing cobalt atoms are situated within virgin C_{60} molecules and following 2 MeV He^+ ion beam treatment does not destroy those except ionization. Indeed, the destruction of the carbon cages will suppress the dopant loss effect owing to damaging the spacious channels and much efficient bonding cobalt with carbon cage fragments [26]. Completely disordered carbon structure will keep cobalt without losing, as it was shown during RBS analysis of the as-implanted samples (Fig. 2b).

The explanation also suggests that 5.5 keV O_2^+ ions, used during the SIMS analysis of potassium-implanted fullerene [10], also leads to ionization of the C_{60} molecules, adjoining the sputtering layer. However, relatively low energy of the oxygen ions implies small thickness of the adjoining C_{60} layer affected during SIMS sputtering. Moreover, the destruction of the carbon cages due to the collisions with oxygen ions should be expected [27]. As a result, a quantity of the dopant loss in that report is found to be much lower compared with the present results, where the C_{60} cage ionization dominates within whole thickness of the fullerene film. Additionally, the difference in the dopant loss is related also with portion of the metal atoms, penetrating into virgin C_{60}. Thus, during the experiments with potassium implantation at the temperature of 300 °C only part of the dopant has penetrated into undestroyed fullerene [10], whereas after the annealing of cobalt-implanted samples all Co atoms are in the C_{60} crystals.

In conclusion, we report on the original method of planar doping of C_{60} crystalline film with metals, using a conventional ion implantation and subsequent annealing. It was shown that cobalt, prior implanted into C_{60} film, moves from the surface a-C layer into the deeper layer of virgin C_{60} due to the annealing at 300 °C temperature. This in-depth cobalt motion is coursed by the carbon density gradient, arising due to ion implantation. Relatively low thermal diffusion ($D = 2 \times 10^{-18}$ cm^2/s) emphasizes the dominant role of the driving force in this cobalt in-depth translation. Deficit of the dopant, found during ion beam analysis of the annealed samples, we refer to the Coulomb repulsion of positive cobalt ions and C_{60} molecules ionized after irradiation by swift helium ions. The presented method of C_{60} doping also yields a formation of a-C surface layer that could be used as protection of the deeper Co–C_{60} composition from any chemical and mechanical influences in possible devices.

Acknowledgement

Support from Japan Society of the Promotion of Science (Award No. L04545 to VL) is gratefully acknowledged.

References

[1] M.S. Dresselhaus, G. Dresselhaus, P.C. Eklund, Science of Fullerenes and Carbon Nanotubes, Academic Press, London, 1996.
[2] R.C. Haddon, L.E. Brus, K. Raghavachari, Chem. Phys. Lett. 125 (1986) 459.
[3] R.F. Curl, R.E. Smalley, Science 242 (1988) 1017.
[4] R.C. Haddon, A.F. Hebard, M.J. Rosseinsky, D.W. Murphy, S.J. Duclos, K.B. Lyons, B. Miller, J.M. Rosamilia, R.F. Fleming, A.R. Kortan, S.H. Glarum, A.V. Makhija, A.J. Muller, R.H. Eick, S.M. Zahurak, R. Tycko, G. Dabbagh, F.A. Thiel, Nature 350 (1991) 320.
[5] A.F. Hebard, M.J. Rosseinsky, R.C. Haddon, D.W. Murphy, S.H. Glarum, T.T.M. Palstra, A.P. Ramirez, A.R. Kortan, Nature 350 (1991) 600.
[6] K. Tanigaki, T.W. Ebbesen, S. Saito, J. Mizuki, J.S. Tsai, Y. Kubo, S. Kuroshima, Nature 352 (1991) 222.
[7] Stephen P. Kelty, Chia-Chun Chen, Charles M. Lieber, Nature 352 (1991) 223.
[8] R.M. Fleming, A.P. Ramizer, M.J. Rosseinsky, D.W. Murphy, R.C. Haddon, S.M. Zahurak, A.V. Makhija, Nature 352 (1991) 787.
[9] H. Ryssel, I. Ruge, Ion Implantation, John Wiley & Sons, Chichester, 1986.
[10] J. Kastner, H. Kuzmany, L. Palmetshofer, P. Bauer, G. Stingeder, Nucl. Instr. Meth. B (80/81) (1993) 1456.
[11] J. Kastner, H. Kuzmany, L. Palmetshofer, Appl. Phys. Lett. 65 (1994) 543.
[12] Yunlong Cui, Senhao Lin, Tingwen Rong, Jingrong Bao, Jianguo Zhang, Nucl. Instr. Meth. B 100 (1995) 502.
[13] S. Prawer, K.W. Nugent, S. Biggs, D.G. McCulloch, W.H. Leong, A. Hoffman, R. Kalish, Phys. Rev. B 52 (1995) 841.
[14] D. Fink, R. Klett, P. Szimkoviak, J. Kastner, H. Kuzmany, L. Palmetshofer, L.T. Chadderton, L. Wang, Nucl. Instr. Meth. B 108 (1996) 114.
[15] K.L. Narayanan, M. Yamaguchi, N. Dharmarasu, N. Kojima, D. Kanjilal, Nucl. Instr. Meth. B 178 (2001) 301.
[16] J.F. Ziegler, J.P. Biersak, U. Littmark, The Stopping and Range of Ions in Solids, vol. 1, Pergamon, New York, 1985.
[17] L.R. Doolittle, Nucl. Instr. Meth. B 15 (1986) 227.
[18] J.P. Biersack, L.G. Haggman, Nucl. Instr. Meth. 174 (1980) 257.
[19] A.C. Ferrari, J. Robertson, Phys. Rev. B 61 (2000) 14095.
[20] J. Friedel, Dislocations, Pergamon Press, Oxford, 1964.
[21] Steven J. Duclos, Keith Brister, R.C. Haddon, A.R. Kortan, F.A. Thiel, Nature 351 (1991) 380.
[22] J. Opitz, H. Lebius, S. Tomita, B.A. Huber, P. Moretto Capelle, D. Bordenave Montesquieu, A. Bordenave Montesquieu, A. Reinköster, U. Werner, H.O. Lutz, A. Niehaus, M. Benndorf, K. Haghighat, H.T. Schmidt, H. Cederquist, Phys. Rev. A 62 (2000) 022705.
[23] A. Reinköster, B. Siegmann, U. Werner, H.O. Lutz, Radiation Phys. Chem. 68 (2003) 263.
[24] V. Lavrentiev, H. Abe, S. Yamamoto, H. Naramoto, K. Narumi, Mater. Lett. 57 (2003) 4093.
[25] Antonis N. Andriotis, Madhu Menon, George E. Froudakis, Phys. Rev. B 62 (2000) 9867.
[26] Tsuyoshi Kurikawa, Satoshi Nagao, Ken Miyajima, Atsushi Nakajima, Koji Kaya, J. Phys. Chem. A 102 (1998) 1743.
[27] Ryosuke Ookawa, Katsumi Takahiro, Kiyoshi Kawatsura, Fumitaka Nishiyama, Shunya Yamamoto, Hiroshi Naramoto, Nucl. Instr. Meth. B 206 (2003) 175.